

# Molecular gas in Carina - Keyhole

## Group Project Presentation

Authors: Nguyen Thi Yen Binh<sup>1</sup>, Mai Nhu Tin<sup>1</sup>, Do Quoc Trong<sup>1</sup>

Supervisor: Dr. Le Ngoc Tram<sup>2</sup>

Advisors: Prof. Karl Menten<sup>2</sup>, Dr. Friedrich Wyrowski<sup>2</sup>, Mr. Hoang Thanh Dat<sup>2</sup>

<sup>1</sup>University of Science and Technology of Hanoi, 18 Hoang Quoc Viet, Hanoi, Vietnam

<sup>2</sup>Max-Planck-Institut für Radioastronomie, Auf dem Hügel 69, 53121 Bonn, Germany

February 22nd, 2023

USTH Group  
Project

N.T.Y.Binh &  
M.N.Tin &  
D.Q.Trong

Introduction and  
purposes

Theoretical  
backgrounds

Scientific  
method and  
data

Results and  
Discussions

Conclusion and  
further progress

- 1 Introduction and purposes
- 2 Theoretical backgrounds
- 3 Scientific method and data
- 4 Results and Discussions
- 5 Conclusion and further progress

USTH Group  
Project

N.T.Y.Binh &  
M.N.Tin &  
D.Q.Trong

Introduction and  
purposes

Theoretical  
backgrounds

Scientific  
method and  
data

Results and  
Discussions

Conclusion and  
further progress

- 1 Introduction and purposes
- 2 Theoretical backgrounds
- 3 Scientific method and data
- 4 Results and Discussions
- 5 Conclusion and further progress

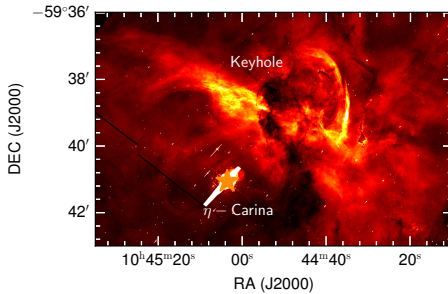
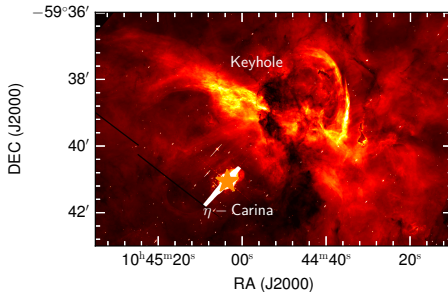


**Figure 1:** Keyhole region seen in  $H_{\alpha}$  by the Hubble Space Telescope <sup>a</sup>.

<sup>a</sup><https://archive.stsci.edu/prepds/carina/datalist.html>



- $\eta$ -Carina belongs to cluster Trumpler 16 (Tr 16), a very strong UV radiation source.

**Figure 1:** Keyhole region seen in  $H_{\alpha}$  by the Hubble Space Telescope <sup>a</sup>.

<sup>a</sup><https://archive.stsci.edu/prepds/carina/datalist.html>

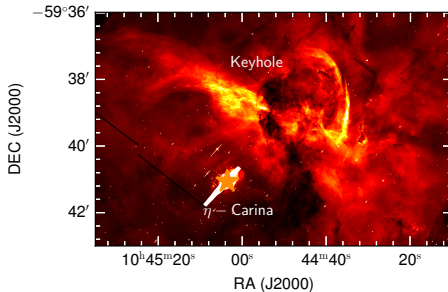


**Figure 1:** Keyhole region seen in  $H_{\alpha}$  by the Hubble Space Telescope <sup>a</sup>.

<sup>a</sup><https://archive.stsci.edu/prepds/carina/datalist.html>

- $\eta$ -Carina belongs to cluster Trumpler 16 (Tr 16), a very strong UV radiation source.
- CO clumps in the cloud nearby Carina, known as a Keyhole (Cox et al. 1995).

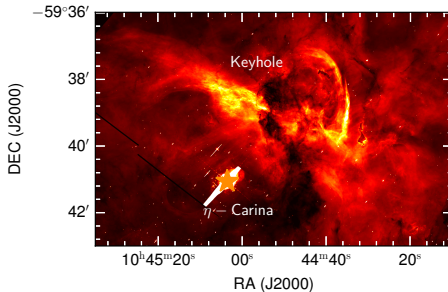


**Figure 1:** Keyhole region seen in  $H_\alpha$  by the Hubble Space Telescope <sup>a</sup>.

<sup>a</sup><https://archive.stsci.edu/prepds/carina/datalist.html>

- $\eta$ -Carina belongs to cluster Trumpler 16 (Tr 16), a very strong UV radiation source.
- CO clumps in the cloud nearby Carina, known as a Keyhole (Cox et al. 1995).  
→ How the molecular gas can survive in the photon-dominated region ?

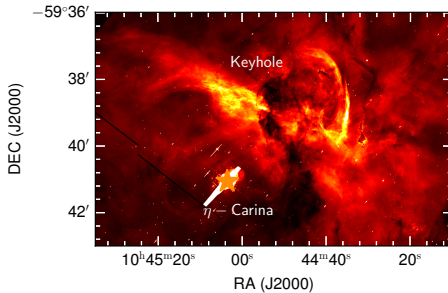


**Figure 1:** Keyhole region seen in  $H_{\alpha}$  by the Hubble Space Telescope <sup>a</sup>.

<sup>a</sup><https://archive.stsci.edu/prepds/carina/datalist.html>

- $\eta$ -Carina belongs to cluster Trumpler 16 (Tr 16), a very strong UV radiation source.
- CO clumps in the cloud nearby Carina, known as a Keyhole (Cox et al. 1995).  
→ How the molecular gas can survive in the photon-dominated region ?  
→ We revisit this region using the new observations from APEX telescope.



USTH Group  
Project

N.T.Y.Binh &  
M.N.Tin &  
D.Q.Trong

Introduction and  
purposes

Theoretical  
backgrounds

Scientific  
method and  
data

Results and  
Discussions

Conclusion and  
further progress

- 1 Introduction and purposes
- 2 Theoretical backgrounds
- 3 Scientific method and data
- 4 Results and Discussions
- 5 Conclusion and further progress

## A molecular cloud

An interstellar gas condensation in which the atoms are bonded together as molecules rather than as free atoms or charged particles.

## A molecular cloud

An interstellar gas condensation in which the atoms are bonded together as molecules rather than as free atoms or charged particles.

- The coldest, densest phase of the interstellar medium.

## A molecular cloud

An interstellar gas condensation in which the atoms are bonded together as molecules rather than as free atoms or charged particles.

- The coldest, densest phase of the interstellar medium.
- Molecules in the interstellar medium are identified by characteristic emission (or absorption) lines in their spectra.

## A molecular cloud

An interstellar gas condensation in which the atoms are bonded together as molecules rather than as free atoms or charged particles.

- The coldest, densest phase of the interstellar medium.
- Molecules in the interstellar medium are identified by characteristic emission (or absorption) lines in their spectra.
- Molecular clouds are the sites of stars formation.

## Photodissociation regions

Photodissociation regions (PDRs) are created by the penetration of far UV (FUV) radiation into molecular clouds.

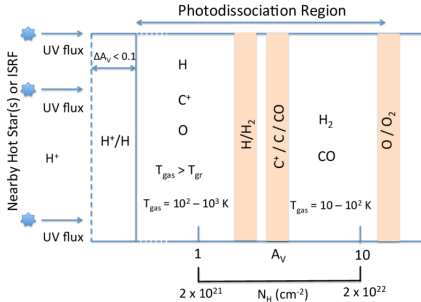


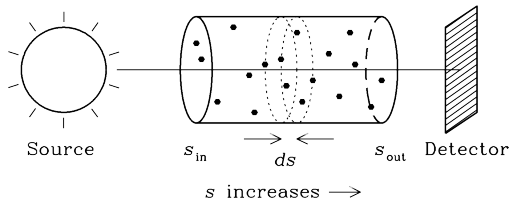
Figure 2: Schematic of a photodissociation regions.

## Radiative transfer equation:

$$\frac{dl_\nu}{ds} = j_\nu - \alpha_\nu l_\nu \quad (1)$$

where  $j_\nu$  is the emission coefficient,  $\alpha_\nu$  is the absorption coefficient.  
Define optical depth as  $d\tau_\nu \equiv \alpha_\nu ds$ , the expression becomes:

$$\frac{dl_\nu}{d\tau_\nu} = S_\nu - l_\nu \quad (2)$$



USTH Group  
Project

N.T.Y.Binh &  
M.N.Tin &  
D.Q.Trong

Introduction and  
purposes

Theoretical  
backgrounds

Scientific  
method and  
data

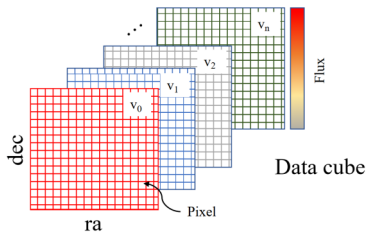
Results and  
Discussions

Conclusion and  
further progress

- 1 Introduction and purposes
- 2 Theoretical backgrounds
- 3 Scientific method and data**
- 4 Results and Discussions
- 5 Conclusion and further progress



- Datacube of  $[^{12}\text{CO}(2-1)]$ ,  $[^{12}\text{CO}(3-2)]$ ,  $[^{13}\text{CO}(2-1)]$ ,  $[^{13}\text{CO}(3-2)]$ ,  $[\text{C}^{18}\text{O}]$  and  $[\text{CI}]$  observed in 2014 by the FLASH and SHeFI receivers on the Atacama Pathfinder EXperiment (APEX) telescope.
- Datacube of  $[^{12}\text{CO}(8-7)]$ ,  $[\text{O I}]$  and  $[\text{N II}]$  measured by the GREAT instrument onboard the Stratospheric Observatory for Infrared Astronomy (SOFIA).
- We combine the archival data of Herschel/PACs at 70 and 160  $\mu\text{m}$ , and Herschel/SPIRE at 250, 350, and 500  $\mu\text{m}$  to build the spectral energy distribution (e.g., flux vs. wavelengths).



The main goal is constraining some of physical properties of Carinae Keyhole such as kinetic temperature and column density by solving radiative transfer equation.

## Local thermodynamic equilibrium (LTE)

LTE (Local Thermodynamic Equilibrium) is an assumption that the radiation field is in thermal equilibrium with the matter in a particular region.

# Physical constraint in LTE condition

- In the LTE conditions, the radiation field of the gas is determined by Planck function and the distribution of the particle population is given by Boltzmann law.

## Radiation temperature $T_R$

$$T_R = f(J_\nu(T_{ex}) - J_\nu(T_{bg}))(1 - e^{-\tau_\nu}) \quad (3)$$

Rayleigh-Jeans Equivalent Temperature:  $J_\nu(T) = \frac{\frac{h\nu}{k}}{e^{\frac{h\nu}{kT}} - 1}$

Excitation temperature:  $T_{ex}$

Beam-filling factor:  $f$

Optical depth:  $\tau_\nu$

Cosmic microwave background:  $T_{bg} = 2.73K$ .

To constrain the total gas column density  $N(H_2)$ , we suggest some assumptions:

- $^{12}CO(2-1)$  is an optically thick line with the value of  $\tau_\nu^{12} \rightarrow \infty$ .
- Excitation temperatures of  $^{12}CO$  and  $^{13}CO$  are the same.
- The abundance ratio of  $\frac{^{12}CO}{^{13}CO} = 65$  and  $\frac{H_2}{^{12}CO} = 10^4$ .

Using the column density, we can derive the gas density, gas mass and visual extinction.

Constraining gas column density  $N_{H_2}$  and dust temperature  $T_{dust}$  based on Spectral Energy Distribution (SED) fitting using dust data of different wavelengths.

## Modified black-body radiation

$$S_\nu = B_\nu(T_d)(1 - e^{-\tau_\nu}) \quad (4)$$

where

Dust optical depth:  $\tau_\nu = \mu_{H_2} m_H \kappa N(H_2)$

Absorption coefficient:  $\kappa = \kappa_0 \left( \frac{\nu}{\nu_0} \right)^\beta$ .

## RADEX

RADEX code <sup>1</sup> is a numerical method for solving non-LTE radiative transfer process in an isothermal and homogeneous medium based on escape probability.

- The program made use of the input format for spectroscopic and collisional data provided by the LAMDA database <sup>2</sup>.
- Using the expanding spherical shell geometry with the escape probability expressed by the following equation:

$$\beta_{LVG} = \frac{1 - e^{-\tau}}{\tau} \quad (5)$$

- We run RADEX model and compare with observed data to constraint kinetic temperature, gas density and column density of emission lines.

<sup>1</sup>Van der Tak et al. 2007

<sup>2</sup><https://home.strw.leidenuniv.nl/moldata/>

## PDR Toolbox

An open-source, science-enabling tool for the community, designed to help astronomers determine the physical parameters of photodissociation regions from observations, developed by M. Wolfire and M. Pound from University of Maryland.

- Model: Wolfire/Kaufman 2006, a plane-parallel model, which is described by a constant H nucleus number density and solves for the chemical balance, thermal equilibrium, and radiation transfer through a PDR layer.
- Input: integrated intensity ( K km s<sup>-1</sup>) of <sup>12</sup>CO(3 – 2), [C I] 609 μm and [C II] 158 μm (Oberst et al. 2011) lines for the region 1.
- Output: Radiation strength and hydrogen nucleus density

## Shielding Effect

Along the line of sight looking from a star, when some molecules are in front of others, the radiation will interact with the front molecules before interacting with the molecules behind. The latter molecules are said to be shielded.

## The shielded photo-dissociation rate <sup>3</sup>:

$$k_i = \chi k_{0,i} \Theta_i \exp(-\gamma A_V) \quad (6)$$

where:

Unshielded rate:  $k_{0,CO} = 2.6 \times 10^{-10} s^{-1}$

Extinction coefficient:  $\gamma = 3.53$

Scaling factor for UV intensity:  $\chi$

Visual extinction:  $A_V$

Shielding function by molecules:  $\Theta$

---

<sup>3</sup>van Dishoeck et al. 2009



## Depth-dependent lifetime

The time needed to fully dissociate a CO cloud or lifetime depends on how many molecules a single line of radiation interacts with. This lifetime is said to be depth-dependent.

## Lifetime of CO cloud:

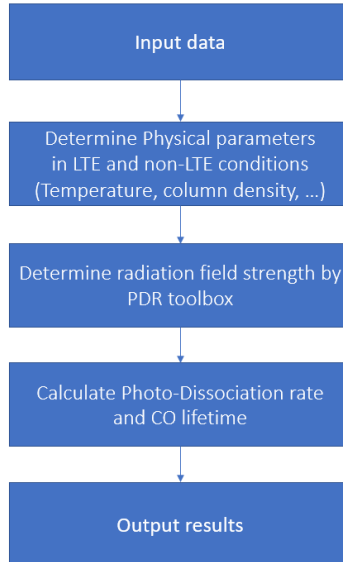
$$t_{PD} = \frac{N(CO) \times d_{reg} \times d_{CO}}{k_{CO}} \quad (7)$$

Column density:  $N(CO)$

Region diameter:  $d_{reg}$

CO diameter:  $d_{CO} = 164 pm$

Shielded photo-dissociation rate:  $k_{CO}$



USTH Group  
Project

N.T.Y.Binh &  
M.N.Tin &  
D.Q.Trong

Introduction and  
purposes

Theoretical  
backgrounds

Scientific  
method and  
data

Results and  
Discussions

Conclusion and  
further progress

- 1 Introduction and purposes
- 2 Theoretical backgrounds
- 3 Scientific method and data
- 4 Results and Discussions**
- 5 Conclusion and further progress

# Integrated Intensity Maps

USTH Group  
Project

N.T.Y.Binh &  
M.N.Tin &  
D.Q.Trong

Introduction and  
purposes

Theoretical  
backgrounds

Scientific  
method and  
data

Results and  
Discussions

Conclusion and  
further progress

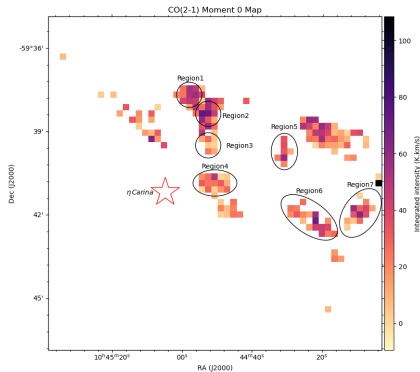


**Figure 3:** Integrated intensity maps of  $^{12}\text{CO}(2-1)$  observed by APEX and our classification of 7 regions. The location of  $\eta$  Carina is symbolised by a star.

- Integrated intensity:  $M_0 = \int I_\nu dv$
- All pixels with the peak value of  $T_{mb} < 3\sigma$  (error) are removed from the map.

# Spectral Lines

USTH Group  
Project

N.T.Y.Binh &  
M.N.Tin &  
D.Q.Trong

Introduction and  
purposes

Theoretical  
backgrounds

Scientific  
method and  
data

Results and  
Discussions

Conclusion and  
further progress

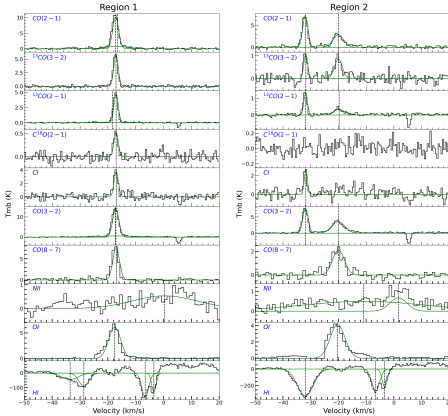


**Figure 4:** Average spectra toward regions 1&2 (black lines). A multi-Gaussian fitting has been deployed (green lines).

**Table 1:** Observational values of CO(2-1) from spectral data.

region	$T_{\text{mb}}^{\text{max}}$ (K)	$\tilde{v}_{\text{LSR}}$ ( $\text{km s}^{-1}$ )	$\sigma_v$ ( $\text{km s}^{-1}$ )
#1	10.41	-17.2	1.04
#2	7.25	-31.93	0.93
	2.86	-19.99	1.90
#3	5.68	-31.92	0.77
#4	2.35	-7.81	1.81
	2.16	9.21	0.90
#5	3.63	-24.84	1.13
#6	2.29	-6.37	0.98
	1.26	-0.73	0.79
#7	3.44	-30.98	0.88

The similarity in peak position and profile of all tracers for position.

**Table 2:** Physical properties constrained by LTE and dust continuum SED fitting.

region	$T_{\text{ex}}$ (K)	$N(\text{H}_2)^{\text{CO}}$ ( $10^{21} \text{ cm}^{-2}$ )	$N(\text{H}_2)^{\text{dust}}$ ( $10^{21} \text{ cm}^{-2}$ )	$A_V$	$M_{\text{gas}}^{\text{CO}}$ ( $M_{\odot}$ )	$M_{\text{gas}}^{\text{dust}}$ ( $M_{\odot}$ )	$n(\text{H}_2)^{\text{CO}}$ ( $10^3 \text{ cm}^{-3}$ )	$n(\text{H}_2)^{\text{dust}}$ ( $10^3 \text{ cm}^{-3}$ )	$T_{\text{dust}}$ (K)
#1	17.45	4.42	5.36	4.70	45.3	54.99	5.60	6.80	36.78
#2	13.99	0.87	4.08	0.93	9.10	42.58	1.10	5.13	38.42
	8.71	1.57	-	1.67	16.38	-	1.97	-	-
#3	12.19	0.41	2.76	0.44	4.69	32.21	0.50	3.34	39.59
#4	8.01	1.02	2.70	1.09	51.98	134.77	0.59	1.56	38.49
	7.74	0.67	-	0.72	33.54	-	0.39	-	-
#5	9.71	1.25	2.81	1.33	62.51	140.09	0.54	1.20	37.71
#6	7.79	0.95	2.90	1.01	57.56	176.06	0.46	1.39	36.11
	6.33	0.40	-	0.42	24.12	-	0.19	-	-
#7	9.46	0.44	2.43	0.47	28.42	155.52	0.33	1.80	34.87

**Notes.** For regions with two peaks (2,4,6), the density of gas derived from dust can be understood that are contributed from both.

**Table 3:** Physical properties constrained by non-LTE constraints.

region	$T_{\text{kin}}$ (K)	$n_{\text{gas}}$ ( $\text{cm}^{-3}$ )	$N(\text{CO})$ ( $\text{cm}^{-2}$ )	$N(\text{H}_2)$ ( $\text{cm}^{-2}$ )
#1	80 - 110	$\sim 10^5$	$2.5 \times 10^{17}$	$2.5 \times 10^{21}$
#2	$\geq 20$	$\geq 10^3$	$\sim 10^{16} - 10^{18}$	$10^{20} - 10^{22}$
	80 - 100	$\sim 10^5 - 5 \times 10^5$	$3 \times 10^{17}$	$3 \times 10^{21}$
#3	$\geq 40$	$\geq 10^4$	$\geq 10^{18}$	$> 10^{22}$
#4	90	$\sim 10^5$	$2.5 \times 10^{17}$	$2.5 \times 10^{21}$
	-	-	-	-
#5	80 - 120	$\sim 5 \times 10^4 - 10^5$	$9 \times 10^{17}$	$9 \times 10^{21}$
#6	$\geq 40$	$\geq 10^4$	$\sim 10^{16} - 10^{18}$	$\sim 10^{20} - 10^{22}$
	$\geq 10$	$\geq 10^3$	$\sim 10^{16} - 10^{18}$	$\sim 10^{20} - 10^{22}$
#7	$\geq 20$	$\geq 10^3$	$\sim 10^{16} - 10^{18}$	$\sim 10^{20} - 10^{22}$

**Notes.** There are no constraints for the second component of region 4 because of missing the CO(3-2) and CO(8-7) lines.

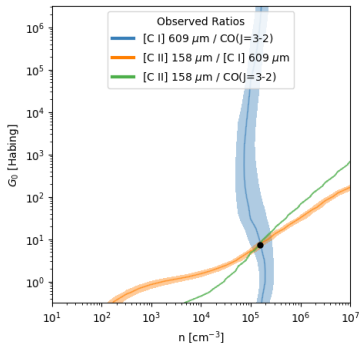


**Figure 5:** Overlay plots show the observed intensity ratios in the  $G_0$  and  $n_H$  grids of the PDR Toolbox. The shaded area represents the observational error.

- $n_H$  is well constrained by the ratio  $609 \mu\text{m} [\text{C I}] / ^{12}\text{CO}(3-2)$ .
- The ratio  $158 \mu\text{m} [\text{C II}]/609\mu\text{m} [\text{C I}]$  and  $158\mu\text{m} [\text{C II}]/^{12}\text{CO}(3-2)$  are helpful for determining the field  $G_0$ .
- The radiation field is just about 7.3 Habing <sup>a</sup> (consistent with Oberst et al. 2011).

$$^a 1\text{Habing} = 1.63 \times 10^{-3} \text{erg cm}^{-2} \text{s}^{-1}$$



# Photo-Dissociation Rate and Dissociated Time

USTH Group  
Project

N.T.Y.Binh &  
M.N.Tin &  
D.Q.Trong

Introduction and  
purposes

Theoretical  
backgrounds

Scientific  
method and  
data

Results and  
Discussions

Conclusion and  
further progress

Table 4: Photo-Dissociation information of each region.

region	$A_V$	$k$ (Molecule $\times s^{-1}$ )	$A_{current}^{CO}$ (Molecules)	$\Delta n_{etacar}^{CO} (*)$ (Molecules)	$t_{PD}$ (Million years)
#1	4.70	$9.022786 \times 10^{-20}$	$5.894959 \times 10^{27}$	0	$2.071731 \times 10^{33}$
#2	0.93	$5.021941 \times 10^{-13}$	$1.171256 \times 10^{27}$	47	$7.395604 \times 10^{25}$
#2	1.67	$2.194837 \times 10^{-13}$	$2.111219 \times 10^{27}$	20	$3.050173 \times 10^{26}$
#3	0.44	$1.027869 \times 10^{-14}$	$5.808129 \times 10^{26}$	9	$1.791809 \times 10^{26}$
#4	1.09	$3.244180 \times 10^{-14}$	$3.283634 \times 10^{27}$	307	$3.209543 \times 10^{25}$
#4	0.72	$5.195587 \times 10^{-14}$	$2.166555 \times 10^{27}$	491	$1.322295 \times 10^{25}$
#5	1.33	$3.270516 \times 10^{-13}$	$3.673553 \times 10^{27}$	31	$3.561750 \times 10^{26}$
#6	1.01	$1.207392 \times 10^{-13}$	$4.107930 \times 10^{27}$	114	$1.078867 \times 10^{26}$
#6	0.42	$2.939979 \times 10^{-13}$	$1.718491 \times 10^{27}$	278	$1.853516 \times 10^{25}$
#7	0.47	$3.413327 \times 10^{-13}$	$1.803640 \times 10^{27}$	32	$1.675580 \times 10^{26}$

Notes.(\*) These values were rounded to the closest integer numbers.

The age of  $\eta - Carina$  is about 3 mil years  $\ll t_{PD}$

$\Rightarrow$  CO clouds survived

## Motion of clouds

Some clouds in considered regions are moving at different velocities indicating these clouds are not in the proximity of  $\eta - Carina$ .

## Number of CO molecules

CO abundance can be inferred by using 3D column density in which the shape of the region hence can be assumed to be spherical.

USTH Group  
Project

N.T.Y.Binh &  
M.N.Tin &  
D.Q.Trong

Introduction and  
purposes

Theoretical  
backgrounds

Scientific  
method and  
data

Results and  
Discussions

Conclusion and  
further progress

- 1 Introduction and purposes
- 2 Theoretical backgrounds
- 3 Scientific method and data
- 4 Results and Discussions
- 5 Conclusion and further progress**

## Conclusions

- Since CO lifetime of each cloud is larger than  $\eta$  – *Carina* lifetime, these observed CO clouds can survive in the proximity of this star.
- Self-shielding and mutual-shielding effects have a strong contribution to reducing the photo-dissociation rate of CO in 7 given regions, hence increasing the lifetime of these clouds.

## Future works

- Indicate the impact of interstellar feedback on our clumps.
- Complete a manuscript to publish.

USTH Group  
Project

N.T.Y.Binh &  
M.N.Tin &  
D.Q.Trong

Introduction and  
purposes

Theoretical  
backgrounds

Scientific  
method and  
data

Results and  
Discussions

Conclusion and  
further progress

**Thank you for listening!**  
Time for questions and defense



---

MAX-PLANCK-GESELLSCHAFT

## Acknowledgment

Thanks to Prof. Karl Menten and Dr. Fried-Rich Wyrowski from Max Planck Institute of Radioastronomy for many considerable supports, contributing to the improvement of our method and resulting in a more plausible conclusion.